NANOSYSTEMS:
PHYSICS, CHEMISTRY, MATHEMATICS

Original article

Shirokikh A.D., et al. *Nanosystems: Phys. Chem. Math.*, 2023, **14** (1), 89–97.
http://nanojournal.ifmo.ru
DOI 10.17586/2220-8054-2023-14-1-89-97

Bioavailability of nanoemulsions modified with curcumin and cerium dioxide nanoparticles

Anastasiya D. Shirokikh[1,a], Viktoriia A. Anikina[2,b], Elizaveta A. Zamyatina[2,c], Ekaterina V. Mishchenko[1,d], Marina Y. Koroleva[1,e], Vladimir K. Ivanov[3,f], Nelli R. Popova[2,g]

[1]Mendeleev University of Chemical Technology, Moscow, Russia

[2]Institute of Theoretical and Experimental Biophysics of the Russian Academy of Sciences, Russia

[3]Kurnakov Institute of General and Inorganic Chemistry of the Russian Academy of Sciences, Moscow, Russia

[a]adshirokikh@gmail.com, [b]viktoriya.anikina@list.ru, [c]sonyoru162@gmail.com, [d]mishchenkoek@list.ru,[e]m.yu.kor@gmail.com, [f]van@igic.ras.ru, [g]nellipopovaran@gmail.com

Corresponding author: Nelli R. Popova, nellipopovaran@gmail.com

ABSTRACT In this work, the physicochemical properties and biological activity of nanoemulsions prepared from paraffin oil and stabilized by nonionic surfactants as carriers of curcumin and cerium dioxide nanoparticles were studied. An analysis of the results showed that curcumin was incorporated into the oil droplets while cerium dioxide nanoparticles were adsorbed on the surface of oil droplets. The nanoemulsion droplet size did not exceed 100 nm. The absence of toxicity to mouse embryonic fibroblasts *in vitro* and after a single intraperitoneal injection to mice *in vivo* makes the nanoemulsions promising drug carriers for advanced biomedical applications.

KEYWORDS nanoemulsions, drug delivery, curcumin, cerium dioxide nanoparticles.

ACKNOWLEDGEMENTS This research has been supported by the Russian Science Foundation (project 22-63-00082).

FOR CITATION Shirokikh A.D., Anikina V.A., Zamyatina E.A., Mishchenko E.V., Koroleva M.Y., Ivanov V.K., Popova N.R. Bioavailability of nanoemulsions modified with curcumin and cerium dioxide nanoparticles. *Nanosystems: Phys. Chem. Math.*, 2023, **14** (1), 89–97.

1. Introduction

Increasing the bioavailability of a number of bioactive compounds of organic and inorganic nature is an urgent task of modern biomedicine. It is well known that some low molecular weight compounds promising for biomedical applications have poor water solubility, which potentially limits their use. Among these compounds, curcumin has a wide range of pharmacological actions, showing anti-inflammatory and antioxidant activity, antimicrobial, wound healing and anticancer properties [1, 2]. Curcumin is a poorly soluble hydrophobic polyphenolic compound of natural origin, having a limited bioavailability. In addition, it has been shown that, under certain conditions, curcumin exhibits cytotoxicity towards normal cells, inducing oxidative stress [3]. Interestingly, when curcumin is combined with cerium oxide nanoparticles (CNP), the latter leveled the toxicity of curcumin against normal cells, due to the inactivation of reactive oxygen species, while retained its action on cancer cells [4, 5]. CNP have unique physical and chemical properties being an inorganic antioxidant performing the functions of some oxidoreductases: catalase, superoxide dismutase and oxidase [6–8]. CNP possess antibacterial, radioprotective [9], regenerative [10] and wound healing properties [11]. CNP nanoemulgel with curcumin shows promise in full-thickness wound healing [12]. Thus, the current research is focused on the development of new curcumin-based formulation, including its complexes with nanoparticles, to increase their bioavailability and therapeutic effects.

To achieve this goal, nanoemulsions (NE) can be used as carrier systems for encapsulating active components, increasing their bioavailability without losing their activity. Particularly relevant is the use of NE to elaborate transdermal and oral delivery systems containing curcumin [13, 14]. NE are kinetically stable disperse systems with droplet sizes up to 100 nm based on a combination of surfactant (cosurfactant), oil and water phases [15]. NE allow the entrapment of a larger quantity of a drug in comparison to conventional topical preparations. The solubility of poorly water-soluble drugs can be increased by NE, in which drugs are dissolved in an oil droplet phase. The penetration of drugs through the diffusional barrier of the skin can also be enhanced by using NE composition [16].

In this work, we obtained NE with paraffin oil, curcumin and CNP and analyzed their properties and toxic effects in *in vitro* and *in vivo* systems.

2. Materials and methods

2.1. Preparation of CeO_2 nanoparticles

The aqueous sol of nanocrystalline cerium oxide stabilized by citrate ions was prepared according to the previously reported protocol [17]. 0.24 g of citric acid was dissolved in 25 ml of 0.05 M aqueous solution of cerium (III) nitrate. This solution was rapidly added to 100 ml of 3 M ammonia solution under stirring and kept for 2 h.

2.2. Nanoemulsion preparation

NE were prepared by low-energy phase inversion temperature method [18]. The mixture of paraffin oil, Tween 60, Span 60 and 0.15 M sodium chloride solution was heated to 95°C under stirring. As a result, a coarse W/O emulsion was produced. This W/O emulsion was quickly cooled in an ice bath under stirring (1000 rpm). Upon cooling, the phase inversion took place and O/W NE were formed. The concentration of the oil phase in NE was 25 vol.%, the surfactant mixture – 12.5 vol.%. The surfactants Tween 60 and Span 60 were taken in a molar ratio of 0.76 [19].

NE with curcumin were prepared. Curcumin (4 wt.%) was dissolved beforehand in paraffin oil, and then NE were prepared as described above (NE+curcumin).

2.3. Modification of curcumin nanoemulsion by cerium dioxide nanoparticles

NE with CNP were produced by mixing of the NE and CNP. Dried citrate-stabilized CNP sol was added to NE with or without curcumin under stirring at 1000 rpm (Fig. 1). Two kinds of NE were ptoduced: NE with CNP (NE+CNP) and NE with curcumin and CNP (NE+curcumin+CNP). The concentration of CNP in both NE was 17.2 mg/ml.

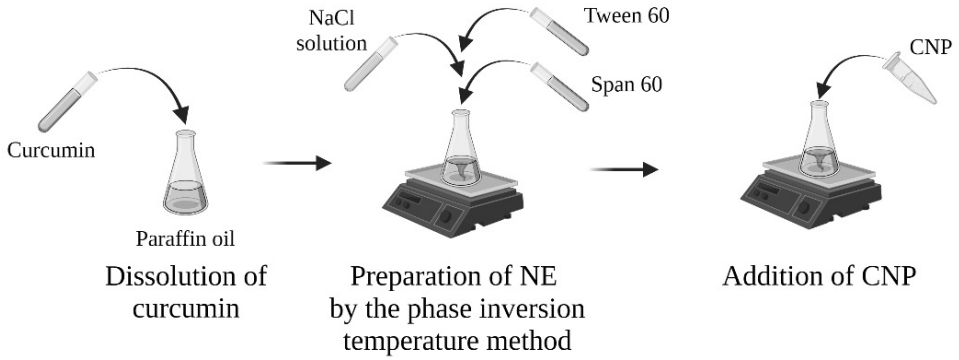

FIG. 1. Scheme of NE modification with curcumin and CNP

2.4. Nanoemulsion droplet size and ζ-potential analysis

The sizes of NE droplets were analyzed by dynamic light scattering technique at an angle of 173° using a helium-neon laser ($\lambda = 633$ nm). The ζ-potential was determined by electrophoretic light scattering method using Zetasizer Nano ZS (Malvern Instruments, United Kingdom). The measurements were carried out at 25°C. Each measurement represented an average of 15 runs (the number of runs was determined automatically by the instrument). The signals were analyzed using a single-plate multichannel correlator coupled to computer equipped with the software package Zetasizer Software for estimating the diameters by the distribution analysis model. All samples were measured at least 5 times; the average measurement error was about 5%.

2.5. Sedimentation stability of nanoemulsions

The sedimentation stability of NE was studied by the analysis of light transmission and backscattering of monochromatic radiation with a MultiScan MS 20 analyser (DataPhysics Instruments GmbH, Germany). The transmitted light was in the near infrared range, the light wavelength was 870 nm. Light transmission and reflection were measured depending on the height of the sample with a measurement resolution of 20 μm. All measurements were carried out at 25°C.

2.6. FTIR- spectroscopy

The Fourier-transform infrared (FTIR) spectra were recorded using a Nicolet 380 (Thermo Fisher Scientific, USA) equipped with a Smart Perfomer single frustrated total internal reflection attachment. The samples were analyzed in the range of 900–4000 cm^{-1} with a resolution of 2 cm^{-1}.

2.7. Cell culture

The Mouse Embryonic Fibroblast (MEF) were cultured in Dulbecco's Modified Eagle's Medium (DMEM)/F12 (1:1) medium with the addition of 10% fetal bovine serum and 100 U/ml penicillin/streptomycin under 5% CO_2 at 37°C.

2.8. MTT assay

The determination of mitochondrial and cytoplasmic dehydrogenases activity in living cells was carried out using a MTT assay based on the reduction of the colorless tetrazolium salt (3-[4.5-dimethylthiazol-2-yl]-2.5-diphenyltetrazolium bromide, MTT). Briefly, different concentrations of the substances (0.0001%, 1%) were added and cells were incubated in a 96-well plate (for 24 h, 48 h and 72 h at 37°C in humid air (98%) containing 5% CO_2). Three hours prior to the end of the exposure period, the supernatant was removed, and MTT (3-(4,5-dimethyl-2-thiazolyl)-2,5-diphenyl-2H-tetrazolium bromide (Sigma-Aldrich, #M5655) solution in phosphate-buffered saline (0.5 mg/mL, 100 μL/well) was added to the cells for 10 min. Upon the completion of the exposure period, the supernatant was removed, and a lysis solution containing 0.1% sodium dodecyl sulfate (Sigma-Aldrich, #L3771) solution in dimethyl sulfoxide was added. Plates were shaken for 5 min, placed on a Multiskan MS Microplate Reader (Thermo Labsystems, Santa Rosa, CA, USA), and the absorbance was read colorimetrically at 570 nm. Each experiment was repeated three times, with four replications.

2.9. Live/Dead assay

Assessment of the viability of the cells cultured in the presence of NE was performed using a Carl Zeiss Axiovert 200 microscope. Cells were seeded into 96-well plates and stained with fluorescent dye Hoechst 33342 (absorption – 350 nm, emission – 461 nm) and a propidium iodide dye (absorption – 493, emission – 636 nm). The dyes were added to the DMEM/F12 without serum (1 μg/ml) and the plate was placed in a CO_2 incubator for 15 min. Microphotographs were taken after washing the cells with a phosphate-buffered saline. For each cell group, four fields in each well were examined. The number of cells (dead/live) was calculated using the ImageJ program.

2.10. Laboratory animals

Animal maintenance was carried out in accordance with the with Directive 2010/63/EU of the European Parliament and of the Council of the European Union on the protection of animals. The experiments were carried out on male white outbred mice (30–35 g), 8–9 weeks old. 12 animals were taken for each group to ensure the validity of the experiment. The animals were hatched and kept in the vivarium of ITEB RAS (Pushchino) by specialized personnel in accordance with the relevant requirements and documentation for the maintenance of laboratory animals. Animals were kept in polycarbonate cages with sawdust bedding, 5 animals each, at a temperature of 22 ± 2°C. Lighting mode was 12h/12h. Animals had free access to water and complete extruded feed for laboratory animals (OOO Laboratorkorm, Russia). Animals with abnormalities detected during the examination were not included in the experiment. Further, all animals were divided into 5 groups. Each animal included in the study was assigned an individual number. Animals were sacrificed after the end of the experiment by the method of cervical dislocation.

2.11. Acute toxicity of the nanoemulsions *in vivo*

The analysis was carried out on outbred white mice with a single intraperitoneal injection of the studied NE at a concentration of 860 mg/kg (10%) in a volume of 0.3 ml/mouse. The initial solutions of the nanoemulsions (NE, NE+CNP, NE+curcumin, NE+curcumin+CNP described above in paragraphs 2.2. and 2.3.) were diluted 10 times with a sterile injection solution (0.15 M NaCl). Control animals were intraperitoneally injected with a sterile injection solution only. All procedures with mice were carried out taking into account the international rules for working with laboratory animals and the requirements of the Commission on Biological Safety and Bioethics of the ITEB RAS (No. 25/2021 dated February 09, 2021). The acute toxicity of the nanocomposites was studied in mice using a 14-day survival test. The general condition of the animals was recorded and reflected in the primary documentation: the characteristics of their behavior, the intensity and nature of motor activity, the presence and nature of convulsions, coordination of movements, skeletal muscle tone, response to tactile, pain, sound and light stimuli, frequency and depth of respiratory movements, condition hair and skin, sensory organs, tail position, amount and consistency of fecal matter, frequency of urination and color of urine.

3. Results and discussion

3.1. Characterization of nanoemulsions

3.1.1. Properties and structure of nanoemulsions with curcumin and cerium dioxide nanoparticles. The size of droplets in NE depends strongly on the method of their preparation. In this work, NE were prepared by temperature phase inversion method. A coarse W/O emulsion was fabricated at elevated temperature. Then this emulsion was rapidly cooled in an ice bath that led to the phase inversion and O/W NE formation. Since the W/O emulsion was initially formed and then it was transformed into O/W one, two surfactants were used in the formulation: Span 60 with low hydrophilic–lipophilic balance (HLB) value and Tween 60 with higher HLB [15].

Our previous study has shown that the solidified shell of the mixture of Tween 60 and Span 60 is formed on the surface of oil nanodroplets at the ambient temperature. This shell provide the efficient protection from coalescence and Ostwald ripening in NE [20, 21]. Curcumin has a lipophilic nature, its molecule contains polar groups that impart amphiphilic

properties. Presumably, curcumin was located near the interface and partly embedded in a surfactant layer of oil droplets in NE.

Biomedical applications require methods for the synthesis of aggregation-resistant nanoparticles stabilized with biocompatible ligands [22–24]. In this work, we used a simple procedure for the synthesis of stable aqueous cerium dioxide sols and studied the effect of the concentration and molar ratio of the initial reagents on the size of CeO_2 particles [17]. The CNP were very small; the average diameter was 5 ± 1 nm (Fig. 2a). The average diameter of NE droplets without curcumin and CNP was 55 ± 5 nm (Fig. 2b). Incorporating CNP in the NE led to increasing the droplet size to 63 ± 5 nm. This increase in an average size indicates that CNP were adsorbed on the surface of the droplet with the formation of an outer solid shell as in the Pickering emulsions [25].

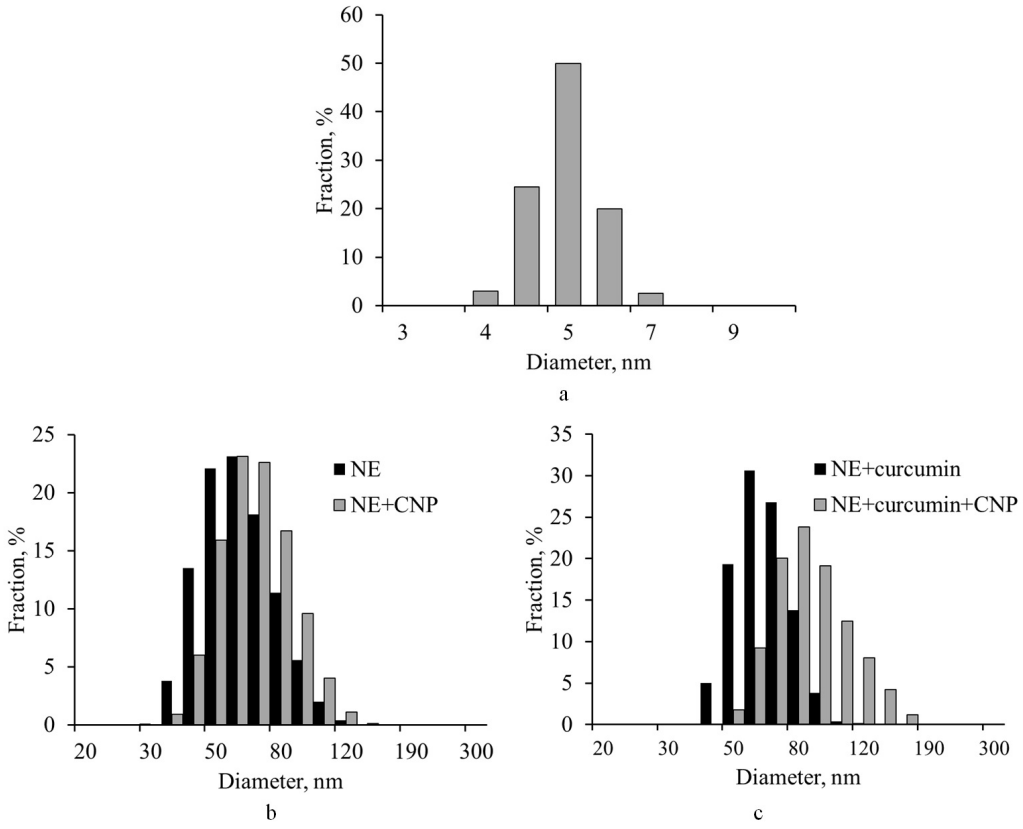

FIG. 2. Size distributions of CNP (a) and droplet size distributions in NE with CNP (b), CNP and curcumin (c)

The addition of curcumin in the lipid phase of NE gave a slight rise in the droplet size to 58 ± 5 nm (Fig. 2b). Modification of the droplets with CNP led to an increase in the droplet diameter up to 78 ± 5 nm, and droplet size distribution became wider. Presumably, in these NE a denser shell of CNP was formed.

CNP were highly charged, ζ-potential was negative and equal to $-(57 \pm 4)$ mV (Table 1). In turn, NE were stabilized with nonionic surfactants. Thus, the ζ-potential of the oil droplets was low and did not exceed $-(2 \pm 1)$ mV. In the presence of curcumin with amphiphilic properties, ζ-potential of oil droplets slightly increased in absolute value.

ζ-potential of oil droplets in NE with CNP was higher in absolute value than in NE without nanoparticles. However, the charge of oil droplets with CNP was lower than the charge of individual CNP partial screening charges of nanoparticles adsorbed on the surface of oil droplets.

The potential curves were derived using the equation presented in [26]. Fig. 3 shows that the potential barrier value was rather low (less than 4 kT) in the suspension of CNP in spite of high value of ζ-potential. In the case of interaction of oil droplet and CNP, the potential barrier was absent. These results indicate that CNP can adsorb on the surface of oil droplets with the formation of nanoparticle shell.

The proposed structure of NE droplets containing CNP is shown in Fig. 4. CNP, being absorbed on the surface of oil droplets in NE, formed a shell that prevented oil droplet flocculation. Due to the high surface charges of CNP, they were presumably located on the surface of oil drops at a small distance from each other. The effect of adsorbed nanoparticles on NE stabilization was confirmed by the long-term stability analysis of such systems. During storage for more than 30 days, all studied NE were stable and no phase separation was observed.

TABLE 1. ζ-potentials of NE droplets with curcumin and CNP

Sample	ζ-potential, mV
NE	-2 ± 1
NE+curcumin	-7 ± 1
CNP	-57 ± 4
NE+CNP	-16 ± 2
NE+curcumin+CNP	-38 ± 3

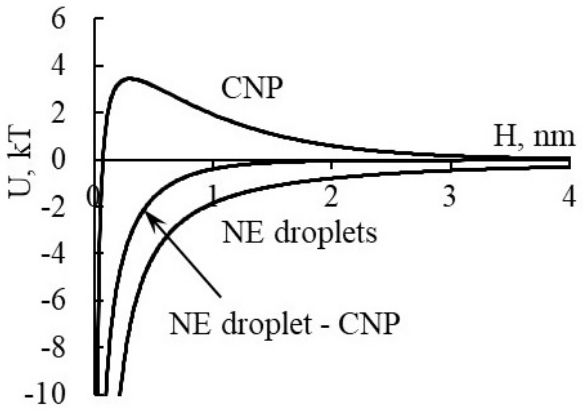

FIG. 3. Potential energy curves of oil droplets in NE, CNP and interaction of oil droplets and CNP

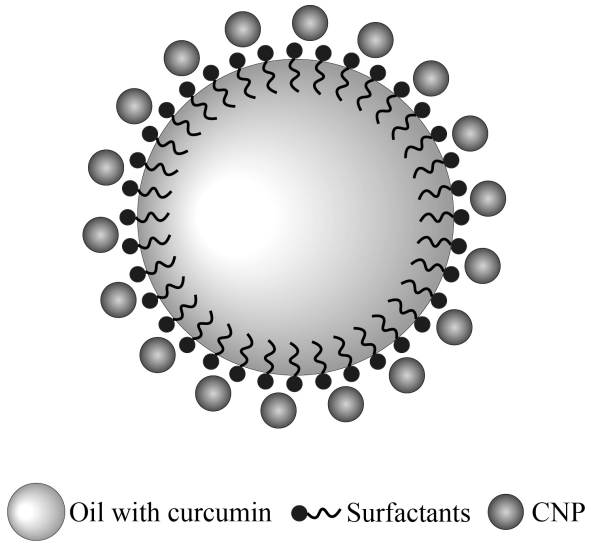

FIG. 4. Schematic representation of the structure of the NE drop with adsorbed CNP

3.1.2. FTIR spectroscopy. In order to confirm the incorporation of active components into the droplets and the absence of chemical interaction between them, FTIR spectroscopy study was carried out. The FTIR spectra (Fig. 5) contained the peaks corresponding to vibrations of the functional groups of the NE components. There were peaks characteristic of alkanes, which corresponded to paraffin oil at 1370 (–CH_3 stretching vibrations), 1470, 2850, 2915 (–CH_2^- stretches) cm^{-1}. The peaks at 950 and 2850 cm^{-1} corresponded to vibrations of C–H bonds in aliphatic compounds. The peaks at 1100 and 1150 cm^{-1} were characteristic of heterocycles of the furan series and C–O–C-group. The vibration of the OH-group in the FTIR spectra was observed at 3440 cm^{-1}. The peaks at 1635–1700 cm^{-1} corresponded to vibrations of C=O-bond. The stretching vibrations of –C–O-group, located in esters, manifested themselves as a peak at 1350 cm^{-1}. All these groups were presented in both Tween 60 and Span 60. A broad peak with a maximum at 3370 cm^{-1} was attributed to the aqueous phase.

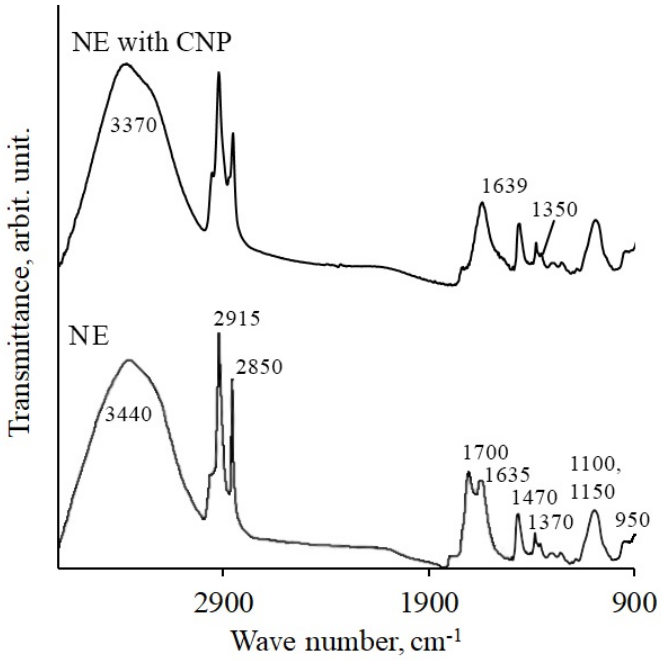

FIG. 5. FTIR spectra of NE without and with CNP

TABLE 2. Data characterizing the toxicity of NE in acute experiments on male SHK mice (intraperitoneally)

Group of animals	Dose, mg/kg	Number of animals			Lethality, %	LD_{50}, mg/kg
		General	Deceased	Survivors		
Control	0	12	0	12	0	Not defined
NE	860	12	0	12	0	Not defined
NE+CNP	860	12	0	12	0	Not defined
NE+curcumin	860	12	0	12	0	Not defined
NE+curcumin+CNP	860	12	0	12	0	Not defined

The presence of peaks, corresponding to NE components, in the FTIR spectra confirmed their incorporation into the droplet structure without chemical alteration.

In the NE containing CNP, an increase in the intensity of the peak at 1639 cm^{-1} was observed, which corresponded to their incorporation in the structure of the NE droplets.

The redox activity of cerium dioxide makes it a promising therapeutic antioxidant [27,28], but the interaction between CNP and NE components can take place in heterogeneous systems. The absence of peak shifts in the FTIR spectra of NE containing CNP indicated the absence of chemical interaction between cerium dioxide and NE components.

3.2. Toxicity of nanoemulsions

3.2.1. Cytotoxicity of the nanoemulsions in vitro. For the cytotoxicity analysis of NE, MEF was used. The metabolic activity of MEF was analyzed by the MTT test after incubation with 4 types of NE:

1 – NE;
2 – NE+CNP;
3 – NE+curcumin;
4 – NE+curcumin+CNP.

At the NE concentrations of 0.0001% and 1% after 24, 48 after 72 h incubation, any significant difference with the control group for 0.0001% NE (Fig. 6) did not reveal. Fig. 6 shows that the metabolic activity of MEF during incubation at 24 and 72 h in the presence of NE at a concentration of 1% with all experimental groups decreased by 40–90% relative to the control group without the addition of NE. In the NE+CNP group after 72 h, the metabolic activity of mouse embryonic fibroblasts increased by 30% relative to the control, which may be due to the presence of CNP in the composition of this emulsion. In the NE+curcumin group after 72 h, there was a decrease in metabolic activity by 15% relative to the control.

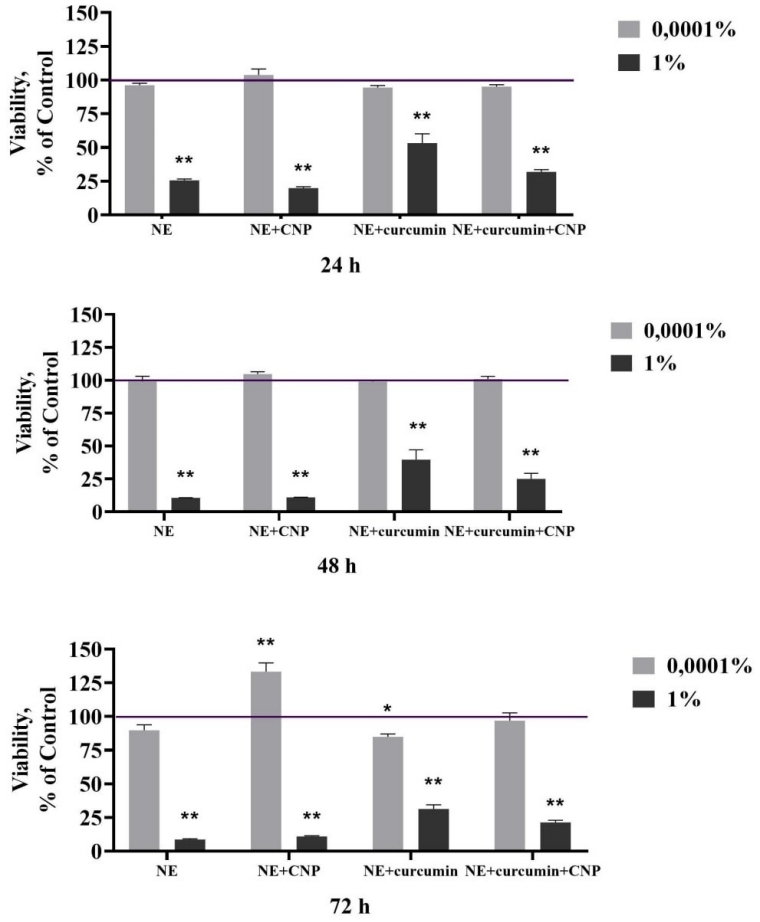

FIG. 6. Metabolic activity (as assessed by MTT assay) of MEF in the presence of NE (0.0001%, 1%) after 24, 48 and 72 h of incubation. Control group line corresponds to the cells that were are not treated with. The data are presented as the mean ±SD. *Significant differences were assessed using the Welch t-test at $0.01 < p < 0.05$ (*), $0.001 < p < 0.01$ (**)

Most probably, this effect was due to the fact that curcumin could be partially segregated on the surface of oil droplets in the NE.

The results of cell viability analysis (Live/Dead assay) by fluorescent staining (all cells – Hoechst 33342 dye, dead cells – propidium iodide) showed that the NE upon incubation during 24, 48 and 72 h with MEF did not have a cytotoxic effect in the concentration range from 0.0001% to 1% (Fig. 7). For the studied NE in the concentration range from 0.0001% to 1%, LD_{50} for the MEF was not detected.

In this way, the incubation of cells with NE at a concentration of 1% led to a decrease in the dehydrogenase activity of cells, which, however, did not lead to a significant increase in cell death compared to the control.

3.2.2. Acute toxicity of the nanoemulsions in vivo. The toxic effect of the NE was assessed by the general condition of the animals and their survival rate. The calculation of surviving and dead animals was carried out within 14 days after the administration of NE, followed by observation of surviving animals for two weeks after intraperitoneal injection. In the first 6 h, the animals were under continuous observation. During the entire observation period, the animals felt normal. Within 14 days of observation of animals, no noticeable deviations were detected in physical activity; the presence of seizures; coordination of movements, the condition of the skin, hair and color of visible mucous membranes; consumption of water and food; body weight.

The results obtained indicate that after a single intraperitoneal injection of NE at a dose of 860 mg/kg in groups of experimental animals, no death of animals was observed during 14 days of the experiment (Table 2). Thus the semi-lethal dose (LD_{50}) could not be determined. A dose of 860 mg/kg was not toxic to mice after a single intraperitoneal injection of NE.

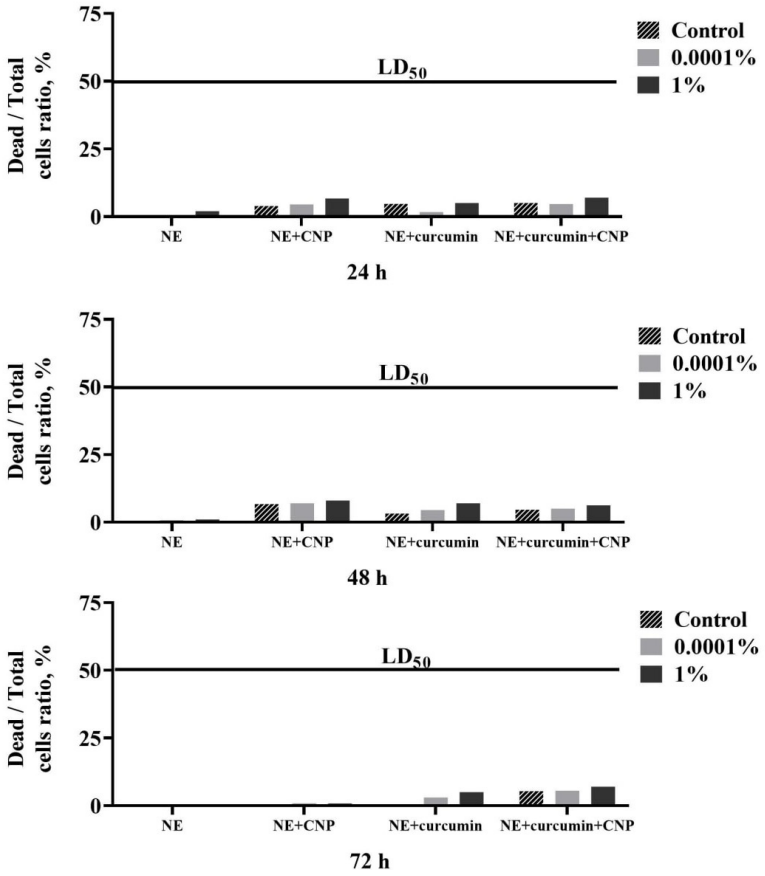

FIG. 7. Live/Dead assay for MEF after 24, 48, 72 h incubation with different concentrations of NE (0.0001%, 1%). Control group line corresponds to the cells that were not treated with. The values are indicated as a percentage of the number of dead cells to their total number

4. Conclusions

In this work, NE with curcumin and cerium dioxide nanoparticles were prepared with droplet sizes less than 100 nm. The absence of a potential barrier in the interaction of oil droplets and CNP makes it possible to impart antioxidant properties to NE. The NE with curcumin and cerium dioxide nanoparticles did not show toxicity to mouse embryonic fibroblasts *in vitro* and after a single intraperitoneal injection in mice *in vivo*. Data obtained demonstrate the possibility of using NE with curcumin and cerium dioxide nanoparticles in advanced biomedical applications.

References

[1] Fitzmaurice S.D., Sivamani R.K., Isseroff R.R. Antioxidant therapies for wound healing: a clinical guide to currently commercially available products. *Skin Pharmacol. Physiol.*, 2011, **24**(3), P. 113–126.

[2] Thomas L., Zakir F., M. Mirza A., Anwer M.K., Ahmad F.J., Iqbal Z. Development of Curcumin loaded chitosan polymer based nanoemulsion gel: in vitro, ex vivo evaluation and in vivo wound healing studies. *Int. J. Biol. Macromol.*, 2017, **101**, P. 569–579.

[3] Lizonova D., Hladek F., Chvila S., Balaz A., Stankova S., Stepanek F. Surface stabilization determines macrophage uptake, cytotoxicity, and bioactivity of curcumin nanocrystals. *Int. J. Pharm.*, 2022, **626**, P. 122133.

[4] Ahsan H., Hadi S.M. Strand scission in DNA induced by curcumin in the presence of Cu (II). *Cancer letters*, 1998, **124**(1), P. 23–30.

[5] Legonkova O.A., Korotaeva A.I., Terekhova R.P., Asanova L.Y., Shcherbakov A.B., Zholobak N.M., Baranchikov A.E., Krasnova E.V., Shekunova T.O., Ivanov V.K. Method for producing a biologically active composite based on nanocrystalline cerium dioxide and curcumin. Patent 2665378. Russia: MPK A61K 31/05. 2017134450, 2018.08.29.

[6] Xue Y., Luan Q., Yang D., Yao X., Zhou K. Direct evidence for hydroxyl radical scavenging activity of cerium oxide nanoparticles. *J. Phys. Chem. C*, 2011, **115**, P. 4433–4438.

[7] Yuao Wu, Hang T Ta. Different approaches to synthesising cerium oxide nanoparticles and their corresponding physical characteristics, and ROS scavenging and anti-inflammatory capabilities. *J. Mater. Chem.*, 2021, **9**(36), P. 7291–7301.

[8] Plakhova T., Romanchuk A., Butorin S., Konyukhova A., Egorov A., Shiryaev A., Baranchikov A., Dorovatovskii P., Huthwelker T., Gerber E., Bauters S., Sozarukova M., Scheinost A., Ivanov V., Kalmykov S., Kvashnina K. Towards the surface hydroxyl species in CeO_2 nanoparticles. *Nanoscale*, 2019, **11**(39), P. 18142–18149.

[9] Popova N.R., Shekunova T.O., Popov A.L., Selezneva I.I., Ivanov V.K. Cerium oxide nanoparticles provide radioprotective effects upon X-ray irradiation by modulation of gene expression. *Nanosystems: Physics, Chemistry, Mathematics*, 2019, **10**(5), P. 564–572.10.

[10] Barker E., Shepherd J., Ortega Asencia I. The Use of Cerium Compounds as Antimicrobials for Biomedical Applications. *Molecules*, 2022, **27**(9), P. 2678.

[11] Popov A.L., Andreeva V.V., Khohlov N.V., Kamenskikh K.A., Gavrilyuk V.B., Ivanov V.K. Comprehensive cytotoxicity analysis of polysaccharide hydrogel modified with cerium oxide nanoparticles for wound healing application. *Nanosystems: Physics, Chemistry, Mathematics*, 2021, **12**(3), P. 329–335.
[12] Singh H., Bashir S.M., Purohit S.D., Bhaskar R., Rather M.A., Ali S.I., Yadav I., Makhdoomi D.M., Din Dar M.U., Gani M.A., Gupta M.K., Mishra N.C. Nanoceria laden decellularized extracellular matrix-based curcumin releasing nanoemulgel system for full-thickness wound healing. *Biomaterials Advances*, 2022, **137**, P. 212806.
[13] Yu H., Huang Q. Improving the oral bioavailability of curcumin using novel organogel-based nanoemulsions. *Journal of agricultural and food chemistry*, 2012, **60**(21), P. 5373–5379.
[14] Ahmad N., Ahmad R., Al-Qudaihi A., Alaseel S.E., Fita I.Z., Khalid M.S., Pottoo F.H. Preparation of a novel curcumin nanoemulsion by ultrasonication and its comparative effects in wound healing and the treatment of inflammation. *RSC advances*, 2019, **9**(35), P. 20192–20206.
[15] Solans C., Solé I. Nanoemulsions: formation by low-energy methods. *Curr. Opin. Colloid Interface Sci.*, 2012, **17**(5), P. 246–254.
[16] Thakkar H.P., Khunt A., Dhande R.D., Patel A.A. Formulation and evaluation of Itraconazole nanoemulsion for enhanced oral bioavailability. *J. Microencapsulation*, 2015, **32**, P. 559–569.
[17] Ivanova O.S., Shekunova T.O., Ivanov V.K., Shcherbakov A.B., Popov A.L., Davydova G.A., Selezneva I.I., Kopitsa G.P., Tret'yakov, Y.D. One-stage synthesis of ceria colloid solutions for biomedical use. *Dokl. Chem.*, 2011, **437**(2), P. 103–106.
[18] Izquierdo P., Esquena J., Tadros Th.F., Dederen C., Garcia M. J., Azemar N., Solans C. Formation and stability of nanoemulsions prepared using the phase inversion temperature method. *Langmuir*, 2002, **18**, P. 26–30.
[19] Koroleva M., Nagovitsina T., Yurtov E. Nanoemulsions stabilized by non-ionic surfactants: stability and degradation mechanisms. *Physical Chemistry Chemical Physics journal*, 2018, **20**(15), P. 10369–10377
[20] Koroleva M., Nagovitsina T., Yurtov E. Properties of nanocapsules obtained from oil-in-water nanoemulsions. *Mendeleev Communications*, 2015, **25**, P. 389–390.
[21] Mun S., McClements D.J. Influence of Interfacial Characteristics on Ostwald Ripening in Hydrocarbon Oil-in-Water Emulsions. *Langmuir*, 2006, **22**, P. 1551.
[22] Lomanova N.A., Tomkovich M.V., Pleshakov I.V., Volkov M.P., Gusarov V.V., Danilovich D.P., Osipov A.V., Panchuk V.V., Semenov V.G. Magnetic characteristics of nanocrystalline bifeo3-based materials prepared by solution combustion synthesis. *Inorganic Materials*, 2020, **56**(12), P. 1271–1277.
[23] Proskurina O.V., Sokolova A.N., Sirotkin A.A., Abiev R.S., Gusarov V.V. Role of hydroxide precipitation conditions in the formation of nanocrystalline BiFeO3. *Russian Journal of Inorganic Chemistry*, 2021, **66**(2), P. 163–169.
[24] Bigall N.C., Rodio M., Avugadda S., Leal M.P., Di Corato R., Conteh J.S., Intartaglia R., Pellegrino T. Scaling Up Magnetic Nanobead Synthesis with Improved Stability for Biomedical Applications. *J. Phys. Chem. A*, 2022, **26**(51), P. 9605–9617.
[25] Chevalier Y., Bolzinger M.A. Emulsions stabilized with solid nanoparticles: Pickering emulsions. *Colloids Surf. A*, 2013, **439**, P. 23–34.
[26] Koroleva M., Yurtov E. Pickering emulsions stabilized with magnetite, gold, and silica nanoparticles: Mathematical modeling and experimental study. *Colloids and Surfaces A: Physicochemical and Engineering Aspects*, 2020, **601**, P. 125001.
[27] Chen B.H., Inbaraj B.S. Various physicochemical and surface properties controlling the bioactivity of cerium oxide nanoparticles. *Critical Reviews in Biotechnology*, 2018, **38**(7), P. 1003–1024.
[28] Celardo I., Traversa E., Ghibelli L. Cerium oxide nanoparticles: a promise for applications in therapy. *Journal of Experimental Therapeutics and Oncology*, 2011, **9**(1), P. 47–51.

Submitted 23 November 2022; accepted 12 December 2022

Information about the authors:

Anastasiya D. Shirokikh – Mendeleev University of Chemical Technology, Department of Nanomaterials and Nanotechnology, Miusskaya sq., 9, Moscow, 125047, Russia; ORCID 0000-0001-7742-7027; adshirokikh@gmail.com

Viktoriia A. Anikina – Institute of Theoretical and Experimental Biophysics of the Russian Academy of Sciences, Institutskaya str., 3, Pushchino, 142290, Russia; ORCID 0000-0002-5028-2064; viktoriya.anikina@list.ru

Elizaveta A. Zamyatina – Institute of Theoretical and Experimental Biophysics of the Russian Academy of Sciences, Institutskaya str., 3, Pushchino, 142290, Russia; ORCID 0000-0002-1275-565X; sonyoru162@gmail.com

Ekaterina V. Mishchenko – Mendeleev University of Chemical Technology, Department of Nanomaterials and Nanotechnology, Miusskaya sq., 9, Moscow, 125047, Russia; ORCID 0000-0003-4443-1569; mishchenkoek@list.ru

Marina Y. Koroleva – Mendeleev University of Chemical Technology, Department of Nanomaterials and Nanotechnology, Miusskaya sq., 9, Moscow, 125047, Russia; ORCID 0000-0002-6931-8434; m.yu.kor@gmail.com

Vladimir K. Ivanov – Kurnakov Institute of General and Inorganic Chemistry of the Russian Academy of Sciences, Leninskiy prosp., 31, Moscow, 119991, Russia; ORCID 0000-0003-2343-2140; van@igic.ras.ru

Nelli R. Popova – Institute of Theoretical and Experimental Biophysics of the Russian Academy of Sciences, Institutskaya str., 3, Pushchino, 142290, Russia; ORCID 0000-0002-0982-6349; nellipopovaran@gmail.com

Conflict of interest: the authors declare no conflict of interest.